European Journal of Physics

PAPER • OPEN ACCESS

A variety of Levitrons: a review

To cite this article: Max Michaelis *et al* 2021 *Eur. J. Phys.* **42** 015001

OPEN ACCESS
IOP Publishing
European Journal of Physics
Eur. J. Phys. **42** (2021) 015001 (13pp)
https://doi.org/10.1088/1361-6404/abbc2c

A variety of Levitrons: a review

Max Michaelis[1,5], Bob Bingham[2,3], Mike Charlton[4] and C Aled Isaac[4,*]

[1] School of Chemistry and Physics, University of KwaZulu-Natal, Durban 4001, South Africa
[2] University of Strathclyde, Glasgow, G4 0NG, United Kingdom
[3] Rutherford Appleton Laboratory, Chilton, Didcot, OX11 0QX, United Kingdom
[4] Department of Physics, College of Science, Swansea University, Singleton Park, Swansea, SA2 8PP, United Kingdom

E-mail: c.a.isaac@swansea.ac.uk

Received 13 May 2020, revised 25 June 2020
Accepted for publication 28 September 2020
Published 12 November 2020

Abstract

After a brief history and critique of some older instruments, several new Levitron geometries are described. As a result of their greater stability these devices can be used as analogues of a number of phenomena and applications, including magnetic resonance techniques, atom traps and accelerator rings. In particular, the notion of the spinning magnet (or spignet) in a linear trap is similar to the mechanism underpinning the confinement of antihydrogen in a magnetic minimum trap, as achieved in experiments at CERN.

Keywords: magnetic levitation, magnetic trapping, antihydrogen, magnetic resonance

S Supplementary material for this article is available online

(Some figures may appear in colour only in the online journal)

1. Introduction

Every child who played with magnets throughout the centuries must have wondered if it were possible to freely suspend one magnet above carefully positioned others. But it was not until 1842 that the Reverend Samuel Earnshaw [1], a 'don' at St. John's College, Cambridge, revealed why this is impossible. In his own words, and considering only inverse square law

*Author to whom any correspondence should be addressed.
[5]Deceased.

forces, 'the instability cannot be removed by arrangement. And consequently, whether the particles be arranged in cubical form, or in any other manner, there will always exist a direction of instability'.

Nevertheless, American inventor Roy M Harrigan succeeded in levitating a spinning magnet of opposite polarity above a dish-shaped magnetic base in 1983 [2], and a device was soon widely marketed under the name 'Levitron'[6] by a company called 'Fascinations'. How Fascinations obtained the right to do this makes absorbing legal reading [3]. Be that as it may, Fascinations did a great job in propagating Harrigan's invention. Even if few people have ever heard his name, thousands had the wonderful experience of seeing a spinning magnetic top, hereafter termed a spignet, hover freely and dance a little above a rectangular magnetic base. They could even pass their hand between the top and the base, or put the floating spignet in a ceramic, glass or aluminium coffee cup, thereby subconsciously learning about the magnetic properties of materials. Incidentally, the name Levitron was itself borrowed from an early plasma physics experiment in which a half ton superconducting ring was levitated inside a vacuum plasma chamber [4].

Early explanations of the Levitron phenomenon which seemed to contradict Earnshaw's theorem were misleading, or at least incomplete. The first complete explanation was propounded by Sir Michael Berry [5] who showed that precession in the magnetic field creates tiny zones of stability—tiny in both senses: space and time. The spatial trap is milli-metric and the stable rotation periods or frequencies have lower and upper limits. Too slow a rotation frequency or spin and the top becomes wildly unstable (not unlike a bullet with too little spin); too high a frequency and the precession is so low that the top becomes subject to Earnshaw's theorem, and it drifts out of the trap. Simon, Heflinger and Ridgway (SHR) [6], gave an excellent and less mathematically challenging 'Levitron tutorial' in the American journal of physics in 1997. They also conducted a series of Levitron experiments to corroborate their derivation of the rotation frequency ranges for a variety of tops. An even simpler derivation of the upper and lower spin limits was given by T B Jones *et al* in the same year [7].

All in all, by the turn of the century, one could have concluded that the Levitron was now but a well understood toy—even if Luis Romero of Sandia Labs [8] did suggest, with copious theoretical support, that it might be possible to operate a horizontal axis levitating device: 'although nobody has used spin-stabilized magnetic levitation for anything other than a scientific toy, it is possible that this principle could in fact have practical applications'. He added that 'it might take an adept experimentalist to build one'.

Since then there has been some progress with standard vertical axis devices and a horizontal axis instrument which will be described in greater detail in section 2. Furthermore, in 2012, the first study of inclined axis Levitrons was published [9] (see figure 1). In this respect, three novel components were essential: a magnetic-V, a pair of outriggers, and a puller, which turned out to be useful in the horizontal Levitron, and in other applications, as discussed in sections 2.2 and 2.3.

The remainder of this article is divided into two main sections: we first briefly report a recent improvement of the vertical axis Levitron (VAL) and the development of a horizontal axis Levitron or HAL. We then describe further educational applications of a variety of Levitrons: this is due to their analogous behaviour to several small and large scale magnetic phenomena. Berry [5] was the first to investigate the analogy between the Levitron and traps for neutral particles such as neutrons or antihydrogen atoms. This was touched upon elsewhere [10], and further discussion is provided here.

[6] By Levitron we mean levitation with permanent magnets, not the powered electronic version sometimes known as Levitronics.

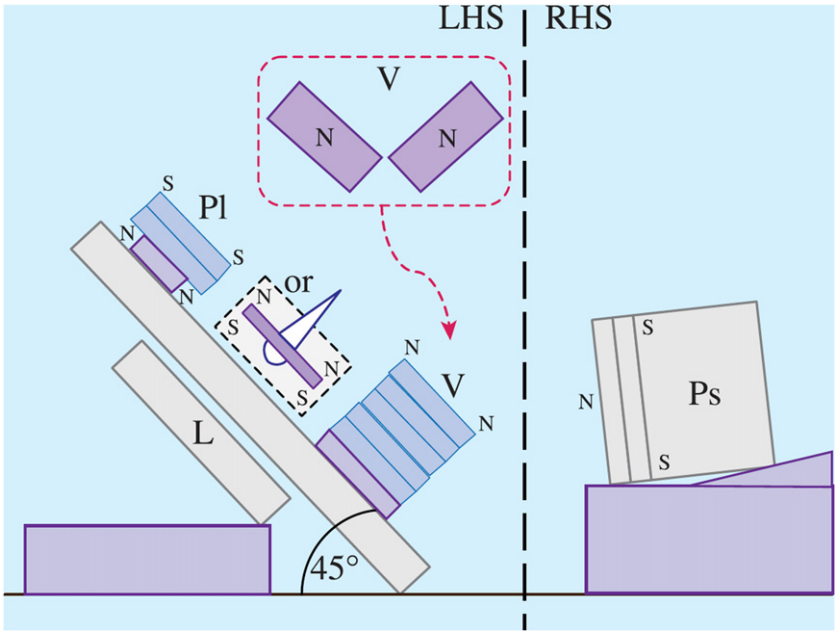

Figure 1. The inclined Levitron experiment of [10]. The stacked puller (Pl) and V-magnets (a pair of stacks oriented in a V-shape as shown on the left-hand side, lhs) were mounted on a sheet of perspex rotated a few degrees from the Levitron base, denoted here by L. The pusher (Ps) magnets on the right-hand side (rhs) allowed the inclination angle of the device to be increased up to about 40°. The outrigger (or) magnets needed on either side of the spignet are also shown. Reproduced from [10].

2. New Levitron experiments

2.1. Vertical axis Levitrons

The VAL is notoriously difficult to run, and it took most users a couple of hours to reliably operate the earliest Fascinations Levitron. Its main difficulty is that little weighting rings are needed to ensure that the spignet remains in the very shallow trap—the latter first explained by Berry [5]. A further major problem is that the magnetism of the base and spignet varies with temperature, such that a configuration that worked in the morning might not later in the same day. A lesser problem is that the vertical alignment is extremely sensitive. Finally, there is the fact that even the slightest draught causes the spignet to escape from the trap. Recently, the company Oxford product design (OPD) and one of us (MM), developed a VAS or 'Hexalev' which is almost fool-proof. A prototype is shown in figure 2. Operation of the Hexalev involved revolving the spignet on a turret, which was then lowered until the spignet detached. The turret could then be adjusted to obtain the best elevation and stability, and then removed to better observe the spignet floating, which it did for nearly two minutes. The turret mechanism contains a small lifting magnet, and as such no weighting rings are needed: and the Hexalev magnetic geometry is easier to level than other Levitrons.

2.2. Horizontal axis Levitrons

In 2012 Michaelis developed a novel HAL geometry which enabled horizontal axis levitation for a few tens of seconds. OPD then improved the device and produced a lightweight version

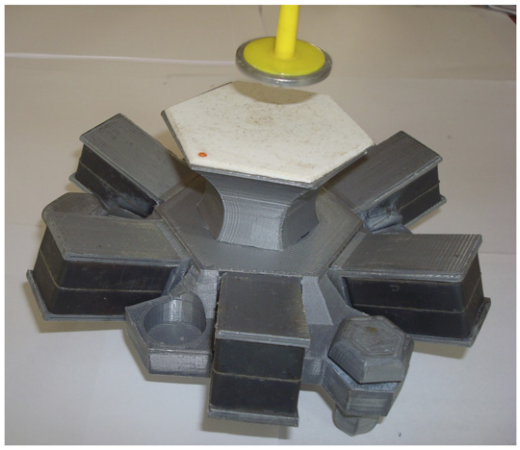

Figure 2. A prototype version of the Hexalev (see text for a description of the operation of the commercial device).

(HALITRON; see, for instance, https://youtube.com/watch?v=AteUnNefRp8) that levitates a spignet for a couple of minutes as with other conventional Levitrons. Since this has been described in some detail in references [10, 11] we only mention here how the HAL relies on two superposed traps, the standard Berry and SHR trap which we term the micro-precessional trap and a macro-trap which gives the spignet much greater stability.

Whereas with a VAL the spignet weight has to be repeatedly adjusted with little rings to compensate for temperature-induced changes of magnetisation, no such adjustment is needed for the HAL: whereas the slightest draught or deliberate puff of air destabilises a VAL, an HAL can be driven by compressed air for as long as necessary. The VAL milli-metric trap becomes centi-metric for the HAL, and there is no need for levelling screws for the base. Most importantly, the increased mechanical stability of the HAL allows one to deliberately destabilise the spignets for a variety of teaching experiments, and possibly for future electro-mechanical applications.

Figure 3 shows a schematic of the field-line geometry of the macro-trap. In [11], we elaborated on the derivation of the SHR stability formulae for the maximum and minimum spin frequencies, which are given by

$$\omega_{\max} = \frac{1}{Ig}\left(\frac{\mu^3 B_0^3}{m}\right)^{1/2} \tag{1}$$

and

$$\omega_{\min} = \frac{2}{I}(\mu B_0 I_t)^{1/2}, \tag{2}$$

and explained why they also apply to the HAL micro-precessional trap. Here I is the moment of inertia of the spignet of mass m and magnetic moment μ, I_t is its moment of inertia around an axis transverse to the main spin axis, B_0 is the magnetic field minimum and g is the local acceleration due to gravity. If one can write $I_t = mr_{\text{eff}}^2$, with r_{eff} some effective radius of the spignet, then from equations (1) and (2), we find

$$\frac{\omega_{\max}}{\omega_{\min}} = \left(\frac{\mu B_0}{2mgr_{\text{eff}}}\right). \tag{3}$$

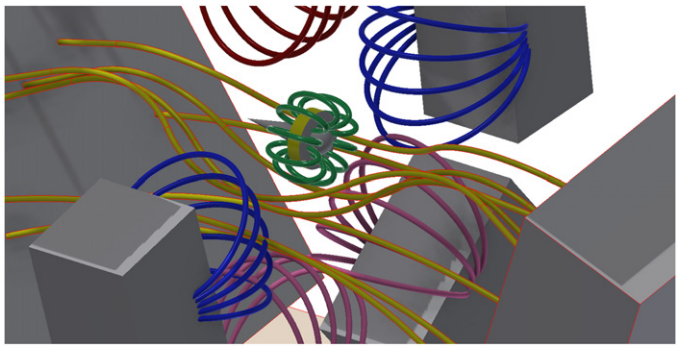

Figure 3. Essential HAL field lines colour coded: the spignet produces the green looped lines and is given support by the mauve lines originating from the 'small-V'; further support is given by the red lines emanating from the puller and which acts like the string of a pendulum. The blue lines emanating from of the outrigger magnets prevent the spignet from escaping sideways and the yellow lines from the 'big-V' create the Berry/SHR micro-precessional trap. (See also the IOP video supplied with [11]).

Since this ratio must clearly be greater than unity for a stable micro-trap, we see the intuitive fact that the magnetic energy of the spignet (μB_0, and see the discussion in section 3.2) should be greater than an effective gravitational potential energy difference ($2mgr_{\text{eff}}$).

Other important equations related to the motions of Levitrons (both vertical and horizontal) are the bounce frequency,

$$\omega_{\text{b}} = \sqrt{\frac{2K\mu}{m}}, \tag{4}$$

with K related to the curvature of the magnetic field (see, for example, [6, 11]), and the precession and nutation frequencies,

$$\omega_{\text{p}} = \frac{\mu B_0}{I\omega} \tag{5}$$

and

$$\omega_{\text{n}} = \frac{\omega I}{I_{\text{t}}}, \tag{6}$$

respectively, where ω is the spignet spin angular frequency. The ratio of these frequencies gives the number, N, of Lissajous-like loops superposed on the precessional motion as

$$N = \frac{\omega_{\text{n}}}{\omega_{\text{p}}} = \omega^2 \frac{I^2}{I_{\text{t}}\mu B_0}. \tag{7}$$

This relationship shows how the number of loops decreases rapidly (and as recently observed [11]) as the spignet slows.

2.3. The flying spignet

Having acquired some knowledge of HAL stability, it became obvious that with stronger magnets the zone of stability could be extended, perhaps allowing the spignet to 'fly'. In reference [11] the flight paths (A), (B), (C) and (D) were described, as shown in figure 4.

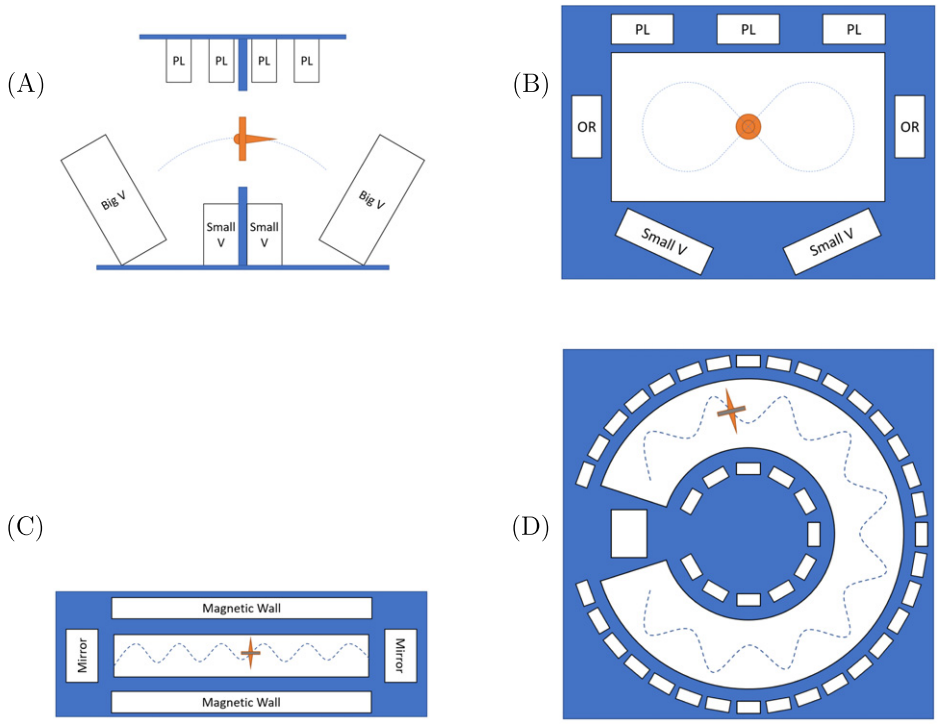

Figure 4. Four flying spignet magnetic geometries. (A) The spignet flies on a circular trajectory from one big-V reflector magnet to the next. (B) Strong puller magnets hold the spignet in the broad window so that it describes a figure eight or generates something like a rosace. (C) The spignet is confined between two straight walls and receives additional lift from a magnetic mat. The linear trajectory is limited by two reflector magnets. (D) A 'magnetic stonehenge' guides the spignet on a circular trajectory. Geometries A and B have been adapted from [11], while (C) and (D) are from more recent, unpublished, work.

(a) In A, the spignet flies axially along the curved field lines from one stronger component of the big-V magnets to the other.

(b) In B, the spignet flies laterally while remaining within the HAL window; it carries out figure eight trajectories as well as more complicated versions. This also requires strengthening and enlarging the small-V magnets. These experiments became possible when it was realised that the large ferrite magnets employed in wind-turbines were affordable, and also could be cut into two pieces (10 cm $\times$ 7 cm $\times$ 2.5 cm) with inexpensive water-jet technology.

(c) The linear trap C (see figure 5—left panel) requires a magnetic mat to be laid between two magnetic walls. The spignet is modified so that it now consists of a symmetric central shaft which is inserted through a hole in the magnetic disc, as shown in figure 5 (right panel). The spignet is spun with two hands and released so that it describes a wavy trajectory. Two magnetic mirrors cause it to travel to-and-fro for a couple of minutes, whereupon the motion becomes transverse and chaotic. This linear trap is relatively compact (18 cm by 8 cm), while the spignet employed is remarkably simple to make and to launch: it consists of a 1.5 cm diameter neodymium perforated disc and a section of cocktail straw.

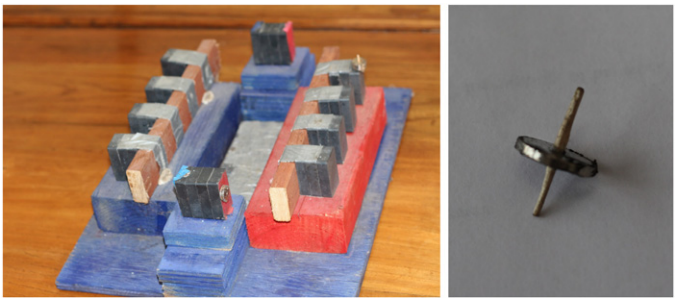

Figure 5. A small linear trap (this one roughly 20 cm in length) with a simple spignet (see text). Linear traps have so far ranged from a metre in length with large spignets, to under 20 cm in length.

(d) A circular version of the linear trap consists of two circular walls and a curved mat. The spignet is launched with the help of a strong reflector magnet which also acts as a target for the spignet when it has completed its circular trajectory. The spignet re-orients itself so as to stick to the launcher magnet.

3. Analogies between Levitrons and various magnetic phenomena

3.1. Magnetic Resonance Imaging

VAL and HAL are both under-appreciated analogues to one of medicine's most important diagnostics: magnetic resonance imaging (MRI). The spignet precession is of the same nature as that of the protons in the strong field of the MRI superconducting solenoid: see the discussions in references [9, 11, 12]. If a laser pointer is directed at the reflecting surface of the spignet (figure 6), interesting Lissajous-like figures appear on a screen (examples are given in figure 7) which show a number of important things common to most freely spinning bodies. The first is that precession is always present, if only barely observable as a tiny loop. If two white points are painted on the spignet and illuminated with a strobe-lamp, the fundamental equation of MRI can be verified. This is equation (5), with the quantised version for MRI being $\omega_{\mathrm{MRI}} = \gamma B_0$ where γ is the gyromagnetic ratio. From equation (5), the precession frequency, as measured with the strobe, is proportional to the magnetic field and inversely proportional to the rotation frequency. For the Levitron spignet in a field of a hundredth of a tesla, the frequency is in the audio range. For the protons in the tesla-level field of an MRI system, the frequency is in the radio-frequency range. In MRI when a burst of radio waves is passed through the patient, the protons resonate and re-emit the waves on a time scale which provides the necessary information to deliver MRI's amazing resolution. This resonance can be imitated with the Levitron in two similar ways: either by placing a small coil next to the Levitron and sending an audio signal through the coil; alternatively, using a small magnet mounted on a variable speed drill to act as a rotary driver. In both cases the precession amplitude increases dramatically if the frequency is matched to the precession frequency.

Furthermore, the same laser pointer and strobe lamp can be employed to introduce some mechanical and space engineering topics: energy and angular momentum of rotational motion; precession and nutation. The HAL could provide a complementary demonstration to the gyroscope. Together with the Berry and SHR theory this is a challenging new topic. The cone of light produced with the laser pointer (which can be visualised by blowing a small amount of smoke) is analogous to the cones described in the well-known mechanical engineering text

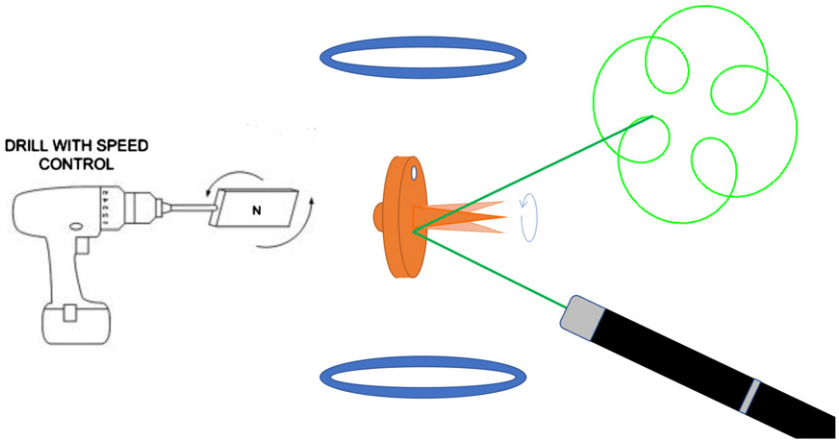

Figure 6. The set up for demonstrating the magnetic precession principle of MRI [9]. The spignet may be held in an HAL or VAL (not shown). A laser pointer produces Lissajous-like loops. The precession and rotation frequencies are measured with a strobe lamp. If a short audio-frequency pulse is passed through the coils (blue), or alternatively the rotary driver is spun at a frequency close to the precessional, the loop amplitude rises dramatically.

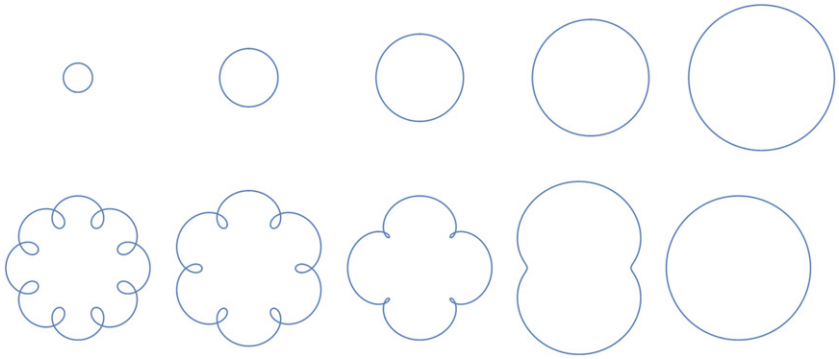

Figure 7. Lissajous-like loops created by shining a pointer beam at the spignet and monitoring the traces on a screen. For an undisturbed Levitron at an early stage of levitation a small precessional loop appears. At a later stage the loop grows—top traces. If the spignet is disturbed, by passing a small magnet in its vicinity or deliberately giving it a 'bad launch', nutation loops are superposed on the precessional (lower traces). Starting with some eight to ten nutation loops, as the spignet slows, the number of loops decreases until a single loop appears just before stability is lost.

by Synge and Griffith [13]. Nutation and precession of spacecraft and solid bodies in space, such as the Earth are a subject of growing practical importance including GPS orientation, spacecraft stabilisation, tumbling space debris, comet rendezvous and space mining: all solid bodies such as exoplanets, and some fluid bodies such as accretion discs, precess and nutate.

3.2. Antimatter traps

It is only relatively recently that antimatter in the form of antihydrogen, the bound state of a positron and an antiproton, has been created in the laboratory (see [14] for a summary) in a

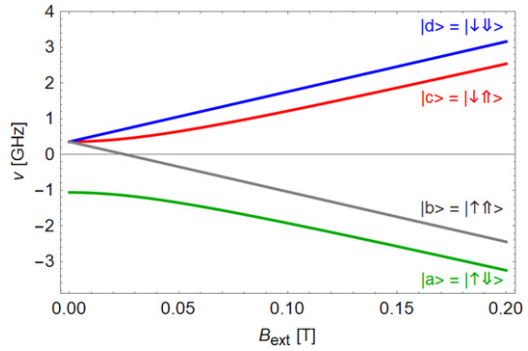

Figure 8. The energy level, so-called Breit–Rabi, diagram of the antihydrogen ground state showing the hyperfine splittings (shown in frequency units of GHz) in a magnetic field, here denoted as $B_{\rm ext}$. The narrow arrows in the states denote the positron spins, while the broad arrows are those of the antiproton: see the text for further discussion.

manner which has allowed it to be held in a trap [15–18]. The traps are direct descendants of those first used to hold atoms [19, 20], and employ a three-dimensional magnetic field minimum to capture a particular population of the anti-atoms. A useful early overview of possible methods for the trapping of charge-neutral species was given by Wing [21], and the basis of magnetic traps in current use has been clearly expounded by Foot (chapter 10) [22].

Trapping can be achieved in a magnetic field, $\boldsymbol{B}$, which is inhomogeneous, since this will exert a force on an atom that possesses a magnetic moment, $\boldsymbol{\mu}$, with the analogous spignet property encountered in section 2.2. The moment–field interaction energy is given by

$$U = -\boldsymbol{\mu} \cdot \boldsymbol{B}, \tag{8}$$

with the corresponding force as

$$\boldsymbol{F} = -\nabla U = \nabla(\boldsymbol{\mu} \cdot \boldsymbol{B}). \tag{9}$$

This can be approximated as $\boldsymbol{F} = \pm|\boldsymbol{\mu}|\nabla|\boldsymbol{B}|$, with $|\boldsymbol{\mu}|$ and $|\boldsymbol{B}|$ the magnitudes of the respective vectors, as long as the rate at which the field experienced by the atom varies as it traverses the trap is much less than the precession frequency of the magnetic moment, $\omega_{\rm L}$, such that

$$\frac{1}{\tau} = \frac{1}{|\boldsymbol{B}|}\left|\frac{{\rm d}\boldsymbol{B}}{{\rm d}t}\right| \ll \frac{\boldsymbol{\mu} \cdot \boldsymbol{B}}{\hbar} = \omega_{\rm L}. \tag{10}$$

This is the so-called adiabatic criterion [23] (sometimes written as $v\frac{\nabla\omega_{\rm L}}{\omega_{\rm L}} \ll \omega_{\rm L}$ [24] where v is a characteristic, typically thermal, speed of the trapped atom) and the Larmor precession frequency has been identified as $\omega_{\rm L} = \boldsymbol{\mu} \times \mathbf{B}/\hbar$. When this condition is valid the magnetic moment adiabatically follows the direction of the field in the trap which means that the centre-of-mass motion can be described classically (see below)[7]. The Larmor frequency identified here is the quantum analogue of equation (5), with $\hbar$ replacing $I\omega$.

For antihydrogen, as hydrogen, in the ground atomic state the magnetic moment is, in the high-field so-called Paschen–Back, limit a constant as

[7] It is implicit in this argument that the magnetic moment is independent of the field. This is not the case at low magnetic fields, as is evident from figure 8 which shows that $\boldsymbol{\mu}$ approaches zero for two of the hyperfine sub-states. We note that the ALPHA atom trap (see text and figure 9) has a 1 T field superimposed which ensures that the assumption of a constant $\boldsymbol{\mu}$ is satisfied.

$$|\boldsymbol{\mu}| = \mu_B = \frac{e\hbar}{2m}, \tag{11}$$

the Bohr magneton, with e and m the electron/positron charge and mass respectively. Thus, the depth scale of the magnetic minimum trap is given by

$$\frac{\mu_B}{k_\mathrm{B}} = 0.67 \ \ \mathrm{KT}^{-1}, \tag{12}$$

with k_B being Boltzmann's constant, such that a field change of 1 T across the dimensions of the trap may confine an antihydrogen atom with a (temperature equivalent) kinetic energy below 0.67 K.

However, there are further considerations pertaining to the magnetic moment of a quantum mechanical object, such as a positron. Unlike the macroscopic spignet, the spin of the particle, which is quantised in multiples of $\hbar/2$, defines the magnetic moment and 'is not an independent parameter' [5]. Thus, for spin 1/2 objects such as electrons and positrons, there are just two (eigen)states with respect to the magnetic field given by the spin quantum number $s = \pm 1/2$, and typically termed 'up' and 'down'. Since the positron spin and the antihydrogen magnetic moment are aligned, it can be seen from equation (8) that $s = -1/2$ (such that $\boldsymbol{\mu}$ and $\boldsymbol{B}$ are opposed) will result a positive U—in other words anti-atoms in such quantum states have an increasing Zeeman energy as the magnetic field increases, and it is these that are potentially trappable.

This is illustrated in figure 8 which shows how the energy levels of ground state antihydrogen are shifted in a magnetic field. Due to the spin combinations of the antiproton and the positron, the atom has both singlet (total spin zero) and triplet (total spin unity) states which are separated at zero field by the hyperfine splitting. This is the ground state maser transition, with a frequency around 1.4 GHz, though known to parts in 10^{13} [25], and which also results in the famous 21 cm wavelength radiation which pervades the Universe. Figure 8 shows the two trappable (low-field seeking) antihydrogen hyperfine states labelled as $|\mathrm{c}\rangle$ and $|\mathrm{d}\rangle$ and the pair of untrapped, high-field seeking, states $|\mathrm{a}\rangle$ and $|\mathrm{b}\rangle$. If transitions can be excited from the trapped to untrapped states by the application of microwave radiation at the required frequencies f_bc and f_ad the positron spins will be flipped, and the antihydrogen will leave the trap and its annihilation may then be detected when it strikes the internal wall of the device. This has formed the basis of some of the recent measurements of the ALPHA antihydrogen collaboration that first detected these transitions [26] and subsequently measured the first anti-atomic spectrum [27]. Such transitions, which took place in a magnetic field of around 1 T in the ALPHA apparatus (see below), are the equivalent of electron spin resonance (or electron paramagnetic resonance), a diagnostic technique which has found wide applications in science. The Breit–Rabi diagram is full of physics: the antiproton $|\mathrm{c}\rangle \rightarrow |\mathrm{d}\rangle$ and $|\mathrm{a}\rangle \rightarrow |\mathrm{b}\rangle$ spin flips are the analogues of the nuclear magnetic resonance transitions at the basis of the MRI technique described briefly in section 3.1.

The magnetic field minimum for neutral atom trapping is realised in three space dimensions using a variant of the so-called Ioffe–Pritchard trap [20, 22]. The configuration of coils used by ALPHA to achieve this is schematically illustrated in figure 9. The axial (z) confinement is provided by the field generated by the mirror coils, while radial capture is effected by the field produced by an octupolar coil system wound directly onto the vacuum chamber housing the charged particle traps. A comparison of figure 9 and the linear spignet device illustrated in figure 5 illustrates the analogy between the atom and spignet traps, with gravity aiding in up-down confinement in the latter, in place of an extra magnetic mat.

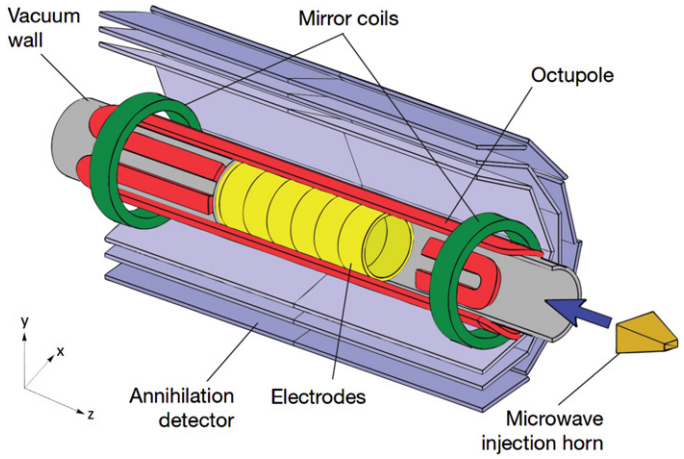

Figure 9. A schematic of the ALPHA apparatus used for antihydrogen trapping and experimentation. The system of coils (in red and green—see text for further discussion) is shown, as well as Penning trap electrodes used for charged (anti)particle confinement which is also effected by the presence of a 1 T magnetic field in the z-direction generated by an external solenoid which is not shown on the diagram. The annihilation detector is a three-layer silicon-based device which can be used to image the antihydrogen/antiproton annihilation position by reconstructing the trajectories of charged pions emitted in the annihilation events. The microwave horn shown can be used to inject microwaves to induce positron spin flip transitions, which de-populate the trap and allow spectroscopic measurements to be undertaken. Reprinted by permission from Springer Nature Customer Service Centre GmbH: [26] Copyright © 2012, Springer Nature.

Antihydrogen is formed in the centre of the trap by the controlled mixing of antiprotons and positrons (see, for example, [28]), and from the considerations above a spin-polarised ensemble, which amounts to about 10^{-3}–10^{-4} of the original anti-atom yield, is captured in a trap about 0.54 K deep. Once captured, the extreme high vacuum inside the apparatus (the Penning trap system—see figure 9—is held at cryogenic temperatures) ensures long survival times [16, 28] such that the antihydrogen can be guaranteed to be in its ground state for experimentation, irrespective of the state in which it was produced.

Despite the differences between the behaviour of classical and quantum spin systems in magnetic traps, their motion while trapped can, in both cases, be described using Newton's laws with the following equation for the motion of the centre of mass position, $\boldsymbol{r}$, of an object (here either the anti-atom, or the spignet) of mass, m, as

$$m\frac{\mathrm{d}^2\boldsymbol{r}}{\mathrm{d}t^2} = \nabla(\boldsymbol{\mu}\cdot\boldsymbol{B}) - mg\hat{\mathbf{y}}, \tag{13}$$

where (in analogy with the antihydrogen trap depicted in figure 9) gravity acts in the y-direction. The behaviour of antihydrogen in the ALPHA field (octupolar–plus–mirror coils) configuration has been analysed in detail [24] in an effort which was crucial in the discussion of the demonstration of a method [29] to use the release of trapped antihydrogen when the magnetic trap is lowered to derive a limit on the gravitational mass of the anti-atom[8].

[8] In a strict Newtonian approach to gravity the 'm' on the left-hand side of equation (13) is the inertial mass of the object, while that in the second term on the right is the gravitational mass: see, for example, [30] for a discussion at the undergraduate level.

Further illuminating work using simulations to analyse the antihydrogen trajectories has recently been completed, revealing that the antihydrogen motion can be characterised as chaotic [31] in ALPHA's octupole trap. In addition, it was found that, following release into the trap, the axial and transverse (see the geometry of the trap in figure 9) kinetic energies were mixed within about 10 s for around two thirds of the trajectories, whereas the remainder do not seem to mix at all. The latter are characterised by having axial kinetic energies lower than about 10% of the total. The spignet trajectories also exhibit complex dynamic behaviour, particularly as the rotation frequency decreases with time (which of course does not occur in quantum systems). It may, though, still be possible to use the spignet, if more controlled experiments can be performed with reproducible starting positions and rotation frequencies, to inform the interpretation of systems such as magnetically trapped antihydrogen, and perhaps other devices using levitating magnetic systems.

4. Conclusions

This article has briefly reviewed Levitron devices, and described several experiments that have demonstrated new capabilities in the horizontal levitation of a spinning magnet using relatively straightforward combinations of permanent magnets. Analogies to other systems, including MRI and trapped antihydrogen, have been examined, and found to be worthy of further exploration.

Acknowledgments

MC and CAI are grateful to the EPSRC for support of their work on low energy antimatter physics. We thank Professor Joel Fajans (UCB) for sharing the results of his antihydrogen trajectory work.

ORCID iDs

Mike Charlton https://orcid.org/0000-0002-9754-1932
C Aled Isaac https://orcid.org/0000-0002-7813-1903

References

[1] Earnshaw S 1842 On the nature of the molecular forces which regulate the constitution of the luminiferous ether *Trans. Camb. Phil. Soc.* **7** 97–112
[2] Harrigan R M 1983 Levitation device *U.S. Patent* 4382245
[3] Sherlock M and Sherlock K 2020 The hidden history of the Levitron http://amasci.com/maglev/lev/expose1.html
[4] Livingston J D 2011 *Rising Force* (Cambridge, MA: Harvard University Press)
[5] Berry M V 1996 The Levitron: an adiabatic trap for spins *Proc. R. Soc.* A **452** 1207–20 10.1098/rspa.1996.0062
[6] Simon M D, Heflinger L O and Ridgway S L 1997 Spin stabilized magnetic levitation *Am. J. Phys.* **65** 286–92
[7] Jones T B, Washizu M and Gans R 1997 Simple theory for the Levitron *J. Appl. Phys.* **82** 883–8
[8] Romero L A 2003 Spin stabilized magnetic levitation of horizontal rotors *SIAM J. Appl. Math.* **63** 2176–94
[9] Michaelis M M 2012 Inclined Levitron experiments *Am. J. Phys.* **80** 949–54

[10] Michaelis M M 2014 Horizontal axis Levitron—a physics demonstration *Phys. Educ.* **49** 67–74
[11] Michaelis M M and Taylor D B 2015 Stability of vertical and horizontal axis Levitrons *Eur. J. Phys.* **36** 065003
[12] Michaelis M M 1983 Permanent magnets help model masers and NMR *Phys. Educ.* **18** 82–4
[13] Synge J L and Griffith B A 1949 *Principles of Mechanics* (New York: McGraw Hill)
[14] Charlton M 2005 Antihydrogen on tap *Phys. Educ.* **40** 229–37
[15] Andresen G B *et al* (ALPHA Collaboration) 2010 Trapped antihydrogen *Nature* **468** 673–7
[16] Andresen G B *et al* (ALPHA Collaboration) 2011 Confinement of antihydrogen for 1,000 seconds *Nat. Phys.* **7** 558–64
[17] Gabrielse G *et al* (ATRAP Collaboration) 2012 Trapped antihydrogen in its ground state *Phys. Rev. Lett.* **108** 113002
[18] Charlton M, Eriksson S, Isaac C A, Madsen N and van der Werf D P 2013 Antihydrogen in a bottle *Phys. Educ.* **48** 212–20
[19] Migdal A L, Prodan J V, Phillips W D, Bergeman T H and Metcalf H J 1985 First observation of magnetically trapped neutral atoms *Phys. Rev. Lett.* **54** 2596–9
[20] Pritchard D E 1983 Cooling neutral atoms in a magnetic trap for precision spectroscopy *Phys. Rev. Lett.* **51** 1336–9
[21] Wing W H 1984 On neutral particle trapping in quasistatic electromagnetic fields *Prog. Quantum Electron.* **8** 181–99
[22] Foot C J 2005 *Atomic Physics, Oxford Master Series in Atomic, Optical and Laser Physics* (Oxford: Oxford University Press)
[23] Golub R and Pendlebury J M 1979 Ultra-cold neutrons *Rep. Prog. Phys.* **42** 439–501
[24] Zhmoginov A I, Charman A E, Shalloo R, Fajans J and Wurtele J S 2013 Nonlinear dynamics of antihydrogen in magnetostatic traps: implications for gravitational measurements *Class. Quantum Grav.* **30** 205014
[25] Essen L, Donaldson R W, Bangham M J and Hope E G 1971 Frequency of the hydrogen maser *Nature* **229** 110–1
[26] Amole C *et al* 2012 Resonant quantum transitions in trapped antihydrogen atoms *Nature* **483** 439–43
[27] Ashkezari M *et al* (ATRAP Collaboration) 2017 Observation of the hyperfine spectrum of antihydrogen *Nature* **548** 66–70
[28] Ahmadi M *et al* (ATRAP Collaboration) 2017 Antihydrogen accumulation for fundamental symmetry tests *Nat. Commun.* **8** 681
[29] Amole C *et al* (ATRAP Collaboration) 2013 Description and first application of a new technique to measure the gravitational mass of antihydrogen *Nat. Commun.* **4** 1875
[30] Tipler P A and Mosca G 2008 *Physics for Scientists and Engineers* 6th edn (New York: W H Freeman and Company) ch 11
[31] Zhong M, Fajans J and Zukor A F 2018 Axial to transverse energy mixing dynamics in octupole-based magnetostatic antihydrogen traps *New J. Phys.* **20** 053003